Chapter 5

Neutron Activation System for ITER Tokamak

Vitaly Krasilnikov, MunSeong Cheon and Luciano Bertalot

Additional information is available at the end of the chapter

http://dx.doi.org/10.5772/intechopen.75966

Abstract

Neutron activation system (NAS) is currently designed for ITER and will be procured by the Korean DA. The main purpose of this diagnostic is to evaluate the integrated fusion power and cross-check with other neutron diagnostic, whose sensitivity can vary over time. Total neutron production rate shall be measured from all over the plasma, regardless of the position or profile of the neutron source. Therefore, it is required to minimize material and its density variation across the field of view between the plasma and the irradiation end.

Keywords: neutron activation system, ITER, nuclear, fusion, tokamak, plasma, diagnostic

1. Introduction

Neutron activation system is a diagnostic measuring the absolute neutron flux and fluence on the first wall [1]. It utilizes pneumatic post method to send a sample of material close to the plasma, where it gets activated by neutrons. This sample is then retrieved back with the same pneumatic post technique and the activation of the sample is measured with gamma-gay spectrometers [2]. The main goal of the ITER neutron activation system (NAS) is to evaluate the total neutron production rate from all over the plasma. The measurement accuracy depends on the position and profile of the plasma and the material in front of the irradiation end. It is required to minimize the amount of material and its density variation across the field of view between the plasma and the irradiation end. Due to the radiation and thermal environment of the ITER in-vessel, however, the measurement from ITER NAS cannot avoid the strong influence from in-vessel materials such as the diagnostic first

wall, blanket modules, and divertor cassettes that are located near the irradiation ends. A number of irradiation positions located above and below the plasma as well as on high-field side and low-field side has been selected for the ITER NAS to compensate the strong influence from in-vessel materials such as the diagnostic first wall, blanket modules, and divertor cassettes.

2. Generic description

ITER NAS measures gamma radiation from samples activated by fusion neutron flux. Encapsulated samples are transferred between irradiation ends and counting station by the driving of nitrogen (or helium) gas. Tubes of diameter 12.7 mm will be used for the transfer lines of the capsule.

NAS consists of the pneumatic transfer system and the counting system (**Figure 1**) Cheon et al. [3]. The pneumatic transfer system includes gas supply, transfer station, transfer line, irradiation ends, counter ends, and disposal bin. It is the subsystem related with the transfer of the encapsulated samples from the loading to the disposal. The PLC-based control system will be harnessed for the accurate operation of the system. The counting system consists of gamma-ray detectors, electronic devices such as high voltage supplies and amplifiers, and tool for neutron source strength evaluation. It is the system for the evaluation of the parameters of the NAS by counting gamma-rays from the activated samples [4].

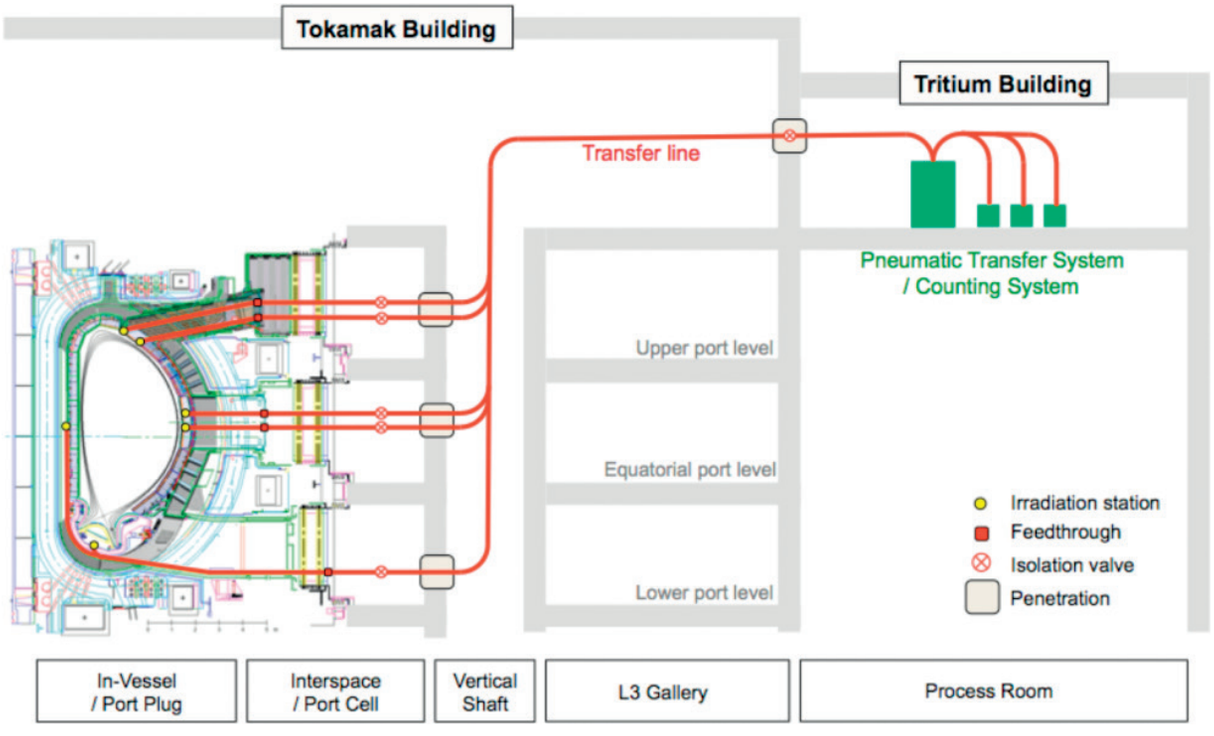

Figure 1. The scheme of neutron activation system for ITER.

http://dx.doi.org/10.5772/intechopen.75966

Due to the large size and the elongated shape of ITER plasma, multiple positions for the irradiation ends in toroidal section are required for highly reliable measurements. At present, four irradiation end locations per toroidal section (A, B, C and D in **Figure 2**) are planned for ITER NAS considering reliability of the measurement and redundancy of the system.

Transfer tubes of the NAS should be bent many times to reach the irradiation ends from the transfer station. To avoid capsule stuck problem around tube bends, there should be a minimum bending radius of the tube in designing tube route. All bends of the tube should have larger radius than this minimum bending radius. Assuming the capsule of OD 8 mm and L 30 mm, and the tube of ID 9 mm, the minimum bending radius of the tube is about 100 mm. The current design value of the minimum bending radius is 150 mm, with the safety factor 50% applied.

Current port allocation for the NAS is #11 and #18 for the upper port, #11 and #17 for the equatorial port, and #12 and #18 for the lower ports. For points A and B, the irradiation ends will be located inside the port plugs. Other irradiation ends will be installed on the vacuum vessel wall with the pipelines routed through the lower level ports [5]. Allocated ports and port numbers for the irradiation locations are shown in **Figure 2**. Total number of the irradiation ends which will be installed is 12.

Transfer station distributes capsules to the appropriate locations such as irradiation end, counting station, or disposal bin. It consists of capsule loader and distribution machine 'carousel.' When capsule is loaded on the carousel from the loader, the platter inside the carousel rotates to place capsule to the point connected to the designated place. The capsule loader and the carousel are separated by the air lock system to prevent the leakage of the driving gas. At every transfer line ends the air cushion technique, which will be implemented to prevent capsule breakage.

Counting station locates outside the bioshield of ITER where neutron flux effect on the detectors is negligible. Detectors such as HPGe or NaI will be used to count gamma-rays from

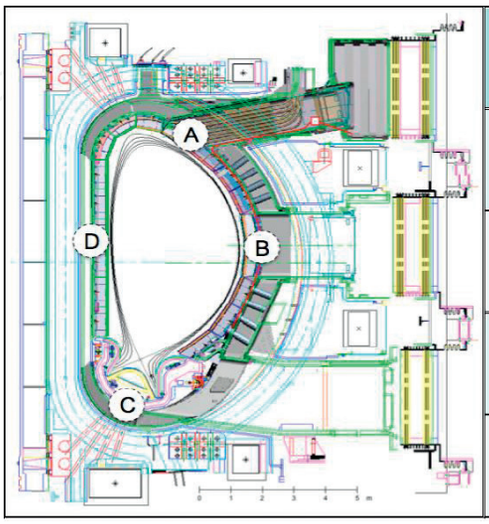

	Port	Port #
A	Upper	#11, #18
B	Equatorial	#11, #17
C	Lower	#12, #18
D	Lower	#12, #18

Figure 2. Distribution of irradiation ends in a toroidal section and allocated port numbers.

the activated samples. The required parameters for the NAS such as neutron fluence will be evaluated from the gamma spectrum considering the location of the irradiation end, sample material and its mass, and irradiation and cooling time.

3. Design of DFW cutout for upper port irradiation end

NAS is supposed to provide reliable and robust measurement data because it will be used for the calibration of other neutron diagnostics. From the point of reliability and robustness of the measurement, optimum location of the irradiation end is where the activation coefficient is insensitive to any environmental changes during the plasma operation and measurement, such as geometrical change of the surrounding material, plasma movement, and slight movement of irradiation end location. The geometrical changes of the irradiation end surrounding material can be happened due to the thermal expansion, vibration, distortion, and so on. Thus, location far away from plasma without any scattering material can be the best place for the irradiation end.

However, materials between the plasma and irradiation end cannot be avoided in real situation. If the location of the irradiation end is far away from the plasma, too much material in-between will increase the measurement uncertainty. On the other hand, if the location of the irradiation end is very close to the plasma, plasma movement will increase the measurement uncertainty as well. So we should find a location where the effect of the plasma movement and the effect of the material are the modest. Normally, an irradiation end without any surrounding material nearby is chosen as the location in given position (by the port location, for example). If the effect of the plasma movement is very significant, compensation of the measurement can be necessary: (1) by using plasma location information from other diagnostics or (2) by measuring simultaneously in the opposite location vertically or radially.

However in ITER, where the radiation environment is extremely harsh, it is very difficult to avoid material around the irradiation end. Instead, we will try to find geometry of the surrounding material, whose impact on the measurement is minimized, with the help of neutron transport calculation.

The irradiation end in the upper port is selected as the object of the investigation because it is one of the locations inside the port plug, where the effect of the geometry change of the surrounding material is less severe than other locations. Most of the in-vessel irradiation ends are located between the blanket shields, where is vulnerable to the geometrical change. The activation coefficients of various samples with and without DFW material have been compared around the irradiation end (see **Figure 4** for instance). The effect of the geometry of the cutout in DFW was investigated to find a design: (1) whose absolute value of the activation coefficient is similar with the one without DFW material and (2) whose response to the plasma movement is not so severe.

Activation coefficients of three samples, that is, silicon, copper, and titanium at the upper port irradiation end were calculated using FISPACT and MCNP code. Objective nuclear reactions are $^{28}Si(n,p)^{28}Al$, $^{63}Cu(n,2n)^{62}Cu$, and $^{48}Ti(n,p)^{48}Sc$.

http://dx.doi.org/10.5772/intechopen.75966

Figure 3 shows the MCNP model for the calculation. The cutout of DFW was designed to have a toroidal and poloidal angle of view as large as possible, while minimizing the amount of material in front of the irradiation end to the plasma direction, in order to minimize errors from the plasma movement and neutron transport calculation. Initial values for each dimension are:

- Depth: 130 mm.
- Poloidal angle: 105°.
- Toroidal angle: 60°.
- Toroidal width: 30 mm.

Calculated activation coefficients are shown in **Figure 4**. When there is no DFW material (upper line) and when there is a cutout in DFW material (lower line). Absolute values of the activation coefficient are reduced by about 10% when the irradiation end is surrounded by

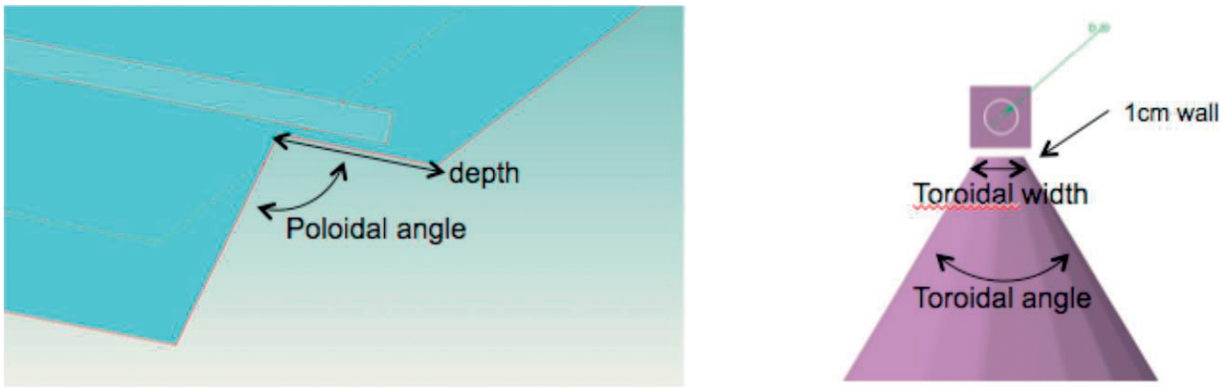

Figure 3. MCNP model for calculation: (left) side view and (right) front view.

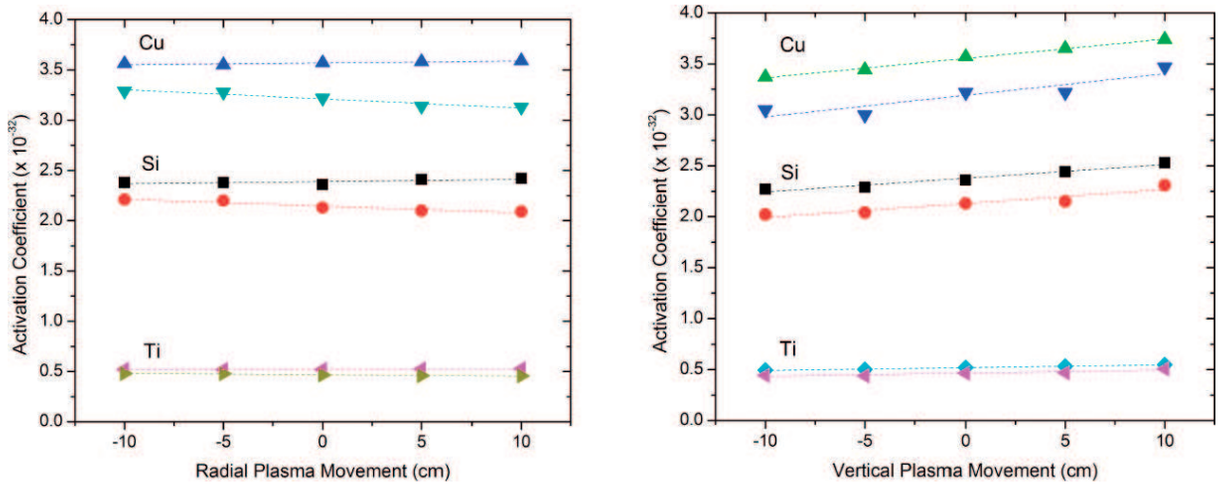

Figure 4. Comparison of plasma movement effect with and without DFW.

DFW material. In spite of the DFW surrounding the response of the irradiation end to the vertical movement of plasma is almost the same with the one without DFW except for the absolute value shift. However, clear decrease of the activation coefficient can be identified when plasma moves outward radially. This can introduce additional error about 2.5% by ±10 cm radial movement of plasma.

Effect of the toroidal width of the cutout was investigated, and the result is shown in **Figure 5**. The width was increased from the initial value (30 mm) up to the geometrical maximum (170 mm) and the activation coefficient of $^{63}Cu(n,2n)^{62}Cu$ reaction was investigated by moving the plasma position in the radial direction. The absolute values of the activation coefficients become closer as the width of the cutout increases. The differences between the 'No-DFW material' case are about 10, 2, and 0.8%, when the widths are 30, 100, and 170 mm, respectively, when the plasma is kept at its central place. Also the response to the plasma

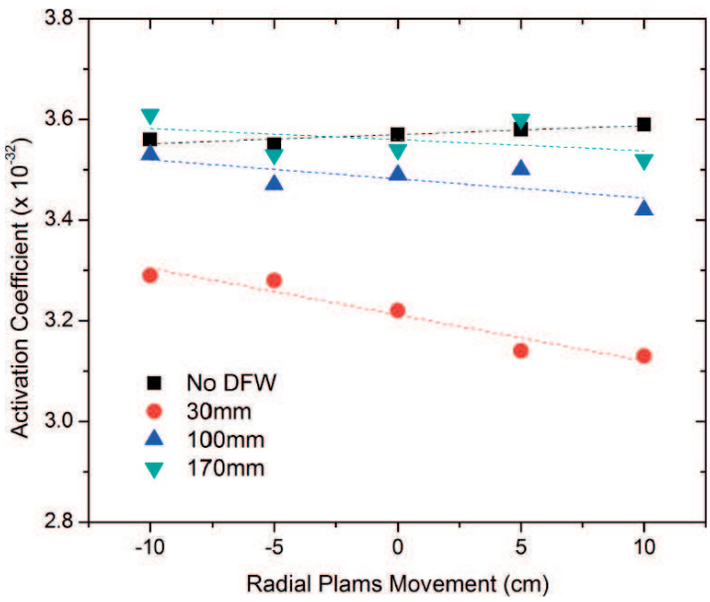

Figure 5. Toroidal width effect on activation coefficients of 63Cu(n,2n)62Cu response by radial plasma movement.

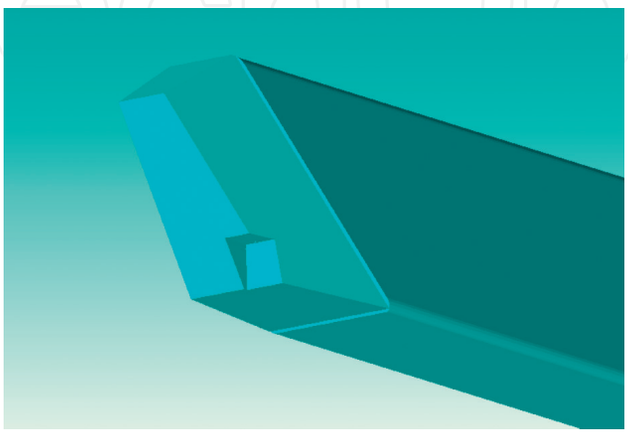

Figure 6. Image of DFW cutout for NAS.

movement is improved by increasing the width. It is easily identified the response of the irradiation end become more insensitive to the plasma movement as the size of the width increases. Slops of the linearly fit equations of the calculated activation coefficients are 9.2, 3.8, and 2.2 ($\times 10^{-34}$) per 1 cm plasma movement, when the widths are 30, 100, and 170 mm, respectively. Calculated maximum errors according to this equation are 0.8 and 1.4%, when the plasma movement values are ±5 cm and ± 10 cm, respectively.

The effect of the DFW cutout design on the measurement accuracy was investigated. The initial design values are proved to be proper except the toroidal width. It is recommended the toroidal width of the cutout to be as large as possible. The recommended design of the DFW cutout is shown in **Figure 6**. By making a cutout according to the design recommended by this calculation, we can imitate as much as possible the response of the ideal irradiation end, where there is no surrounding material nearby.

4. Evaluation of measurement accuracy

Measurement accuracy of NAS with 12 irradiation ends is estimated using MCNP calculations. The response of each irradiation location is evaluated by changing the location and the profile of the neutron source (see **Figure 7**).

The evaluated result of the neutron source displacement effect (**Figure 8**) shows that the upper port is the best position for the irradiation due to its lowest sensitivity. The induced error due to the vertical displacement can be even lower when it is compensated with the measurement at divertor position, as long as the irradiation end at divertor is well characterized during the plasma operation. It is estimated that induced error from the neutron source displacement can be ~ ± 1% even without compensation from other diagnostics, from the simultaneous

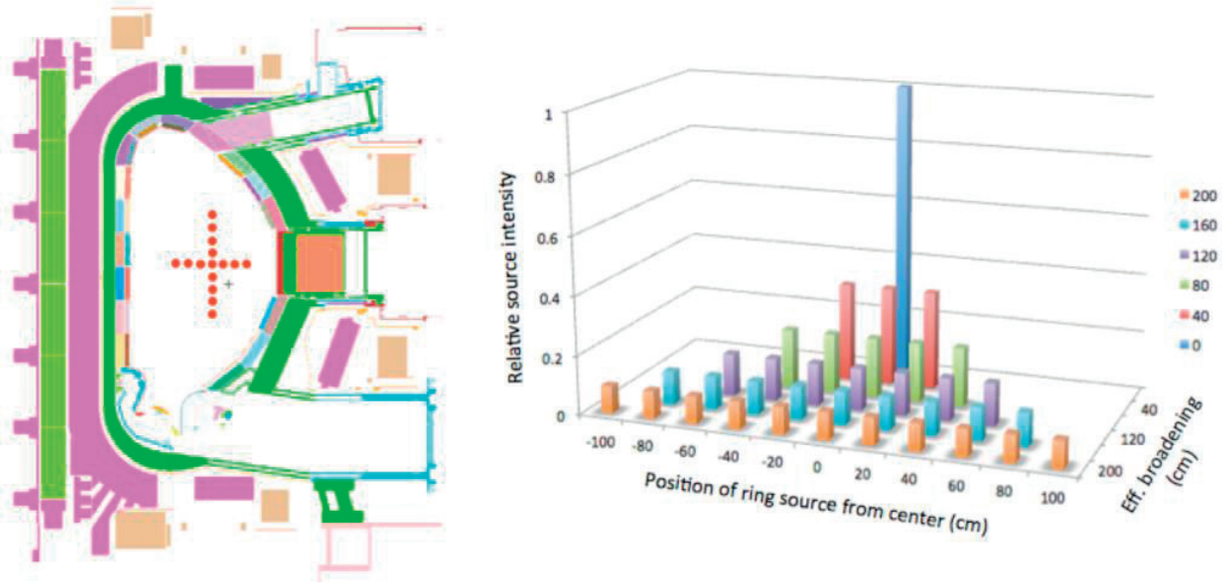

Figure 7. Evaluation of the effect of neutron source position and broadening.

measurement from the upper and divertor position, when the displacement range is within ±20 cm vertically and radially. The equatorial port position can be used for backup when the data are compensated from other diagnostics.

The effect of neutron source broadening (**Figure 9**) on the measurement, which cannot be estimated during the in-vessel calibration, was evaluated. The result also indicates that the upper port is the best position because it has the lowest effect from the neutron source broadening, and shows good characteristic of depending only on the vertical broadening. It is interesting to note that the equatorial port position shows symmetric measurement with the upper port position. Therefore, the simultaneous measurements from the upper and equatorial port position are expected to provide the total neutron production with the broadening error of ~1% without compensation from other diagnostics, when the profile peaking factor is in the range of $3 < \alpha < 7$.

The calculations show that with the combination of the measurements from the upper port, equatorial port, and divertor region can provide relatively good evaluation of the total neutron production in the plasma. In spite of the low reliability of the measurement from the inboard midplain position, it is reasonable to keep this irradiation ends, as they are the only ones capable of providing the absolute value of the neutron flux coming to the inboard side.

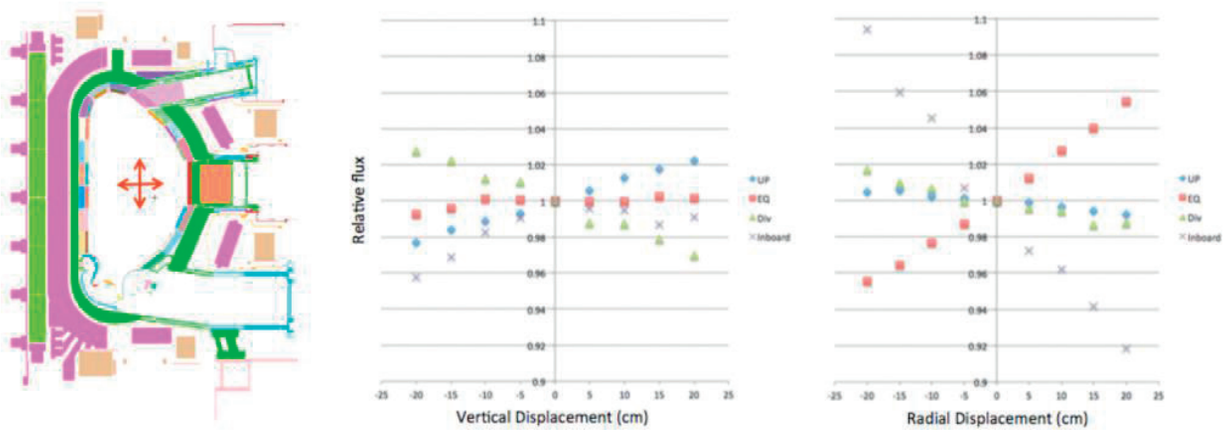

Figure 8. Evaluation of the effect of neutron source position.

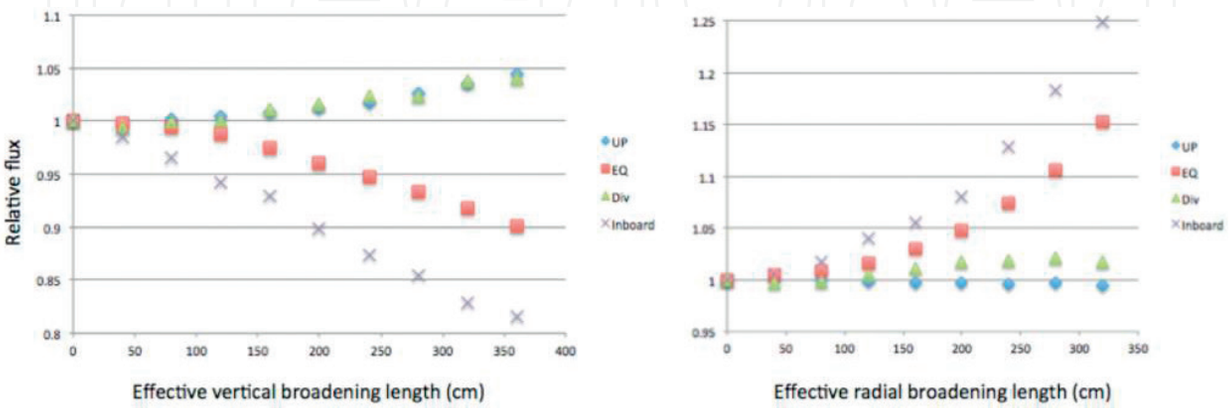

Figure 9. Evaluation of the effect of neutron source broadening.

5. Designs of the NAS components for ITER

Thermal analysis has made significant impact on the design of the NAS front-end components (**Figure 10**). All NAS components installed inside the vacuum vessel shall follow the design guideline SDC-IC (Structural Design Criteria for ITER In-vessel Components), which requires the maximum temperature of the components to be less than about 500°C. According to the simple thermal analysis on the irradiation end in the upper port, the temperature of the irradiation end is found to exceed 500°C when the irradiation end protrudes only by 6 cm from the actively cooled diagnostic shield module (DSM) inside (but not touching) the diagnostic first wall (DFW) that has a full depth of 60 cm. Similarly, all in-vessel irradiation ends located inboard side of the vacuum vessel are found to exceed 500°C, when there is no active cooling of the irradiation end structures. The temperature could be below 500°C only when the forced circulation of He gas with the velocity higher than 10 m/s is provided for the in-vessel transfer line during the plasma operation, which can be problematic when the gas blowing with such velocity fails, for example, when the capsule touches the irradiation location and plugs the hole for the gas circulation. In order to resolve the thermal issue, the design is updated to cool down all in-port irradiation ends by attaching the cooling jacket around the irradiation end structure, where coolant can be supplied from the in-port coolant manifold.

Port plug irradiation ends mainly consist of two transfer lines which are composed of coaxial or parallel tubes (**Figure 11**). Most components will be fabricated with SS316L except the capsule monitoring cabling, which consists of MgO mineral insulated (MI) cables and Al_2O_3-based electrical feedthrough. The front part of the irradiation end is enclosed with the coolant housing, which is connected with the coolant tubing. Two guiding rings are attached on the outside of the coolant housing for the smooth insertion of the irradiation end into the DSM. The feedthroughs will be welded on the closure plate of the port plugs.

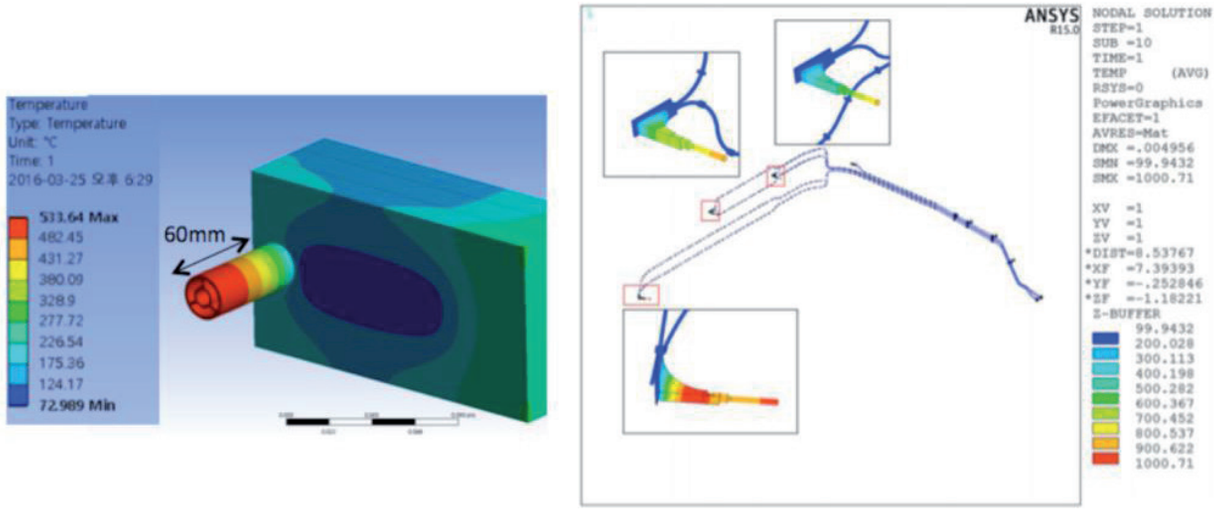

Figure 10. Calculated temperature of NAS irradiation ends.

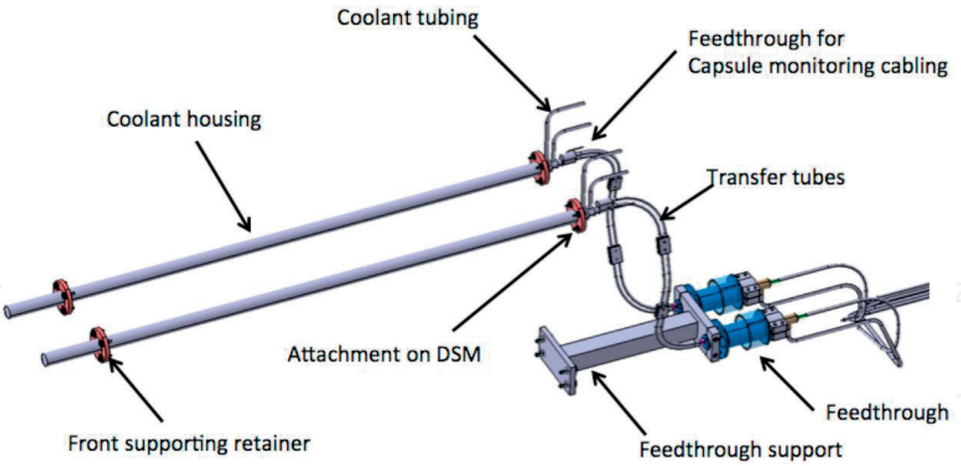

Figure 11. Port plug transfer line in EP11.

Transfer station consists of many moving components such as a servo-motor, linear actuators and many solenoid or gas-driven valves. Pneumatic properties of the transfer system for transferring capsule are as below:

- Pressure of gas in reservoir: ~8 bars max.
- Pressure of driving gas: 1–8 bars
- OD of sample transfer tube: 12.7 mm
- Thickness of sample transfer tube: 1.25 mm
- OD of retrieving gas tube: 12.7 mm
- Thickness of retrieving gas tube: 1.25 mm
- Diameter of capsule: ~8 mm
- Length of capsule: ~20 mm

Samples will be transferred to the designated position by the action of distribution machine 'carousel' (**Figure 12**). Rotating platter inside the carousel will transfer sample to the loading position which are connected to the designated position. When the samples are ready, the valves behind are opened to shoot them to the designated positions. Before arriving at the designated position, the speed of them will be slowed down to prevent breakage. A Programmable Logic Controller (PLC) will control the operation of the transfer system. Figure 9.4.2 is a current design of the carousel.

Counting station measures gamma-rays from the activated samples. It consists of gamma-ray detector, signal processing electronics such as high voltage supply, preamplifier, amplifier, and multichannel analyzer, and data analyzing software. Many gamma-ray detectors such as gas chambers, scintillators, and semiconductor detectors are commercially available. Among these detectors, NaI detectors and HPGe detectors are the most commonly used

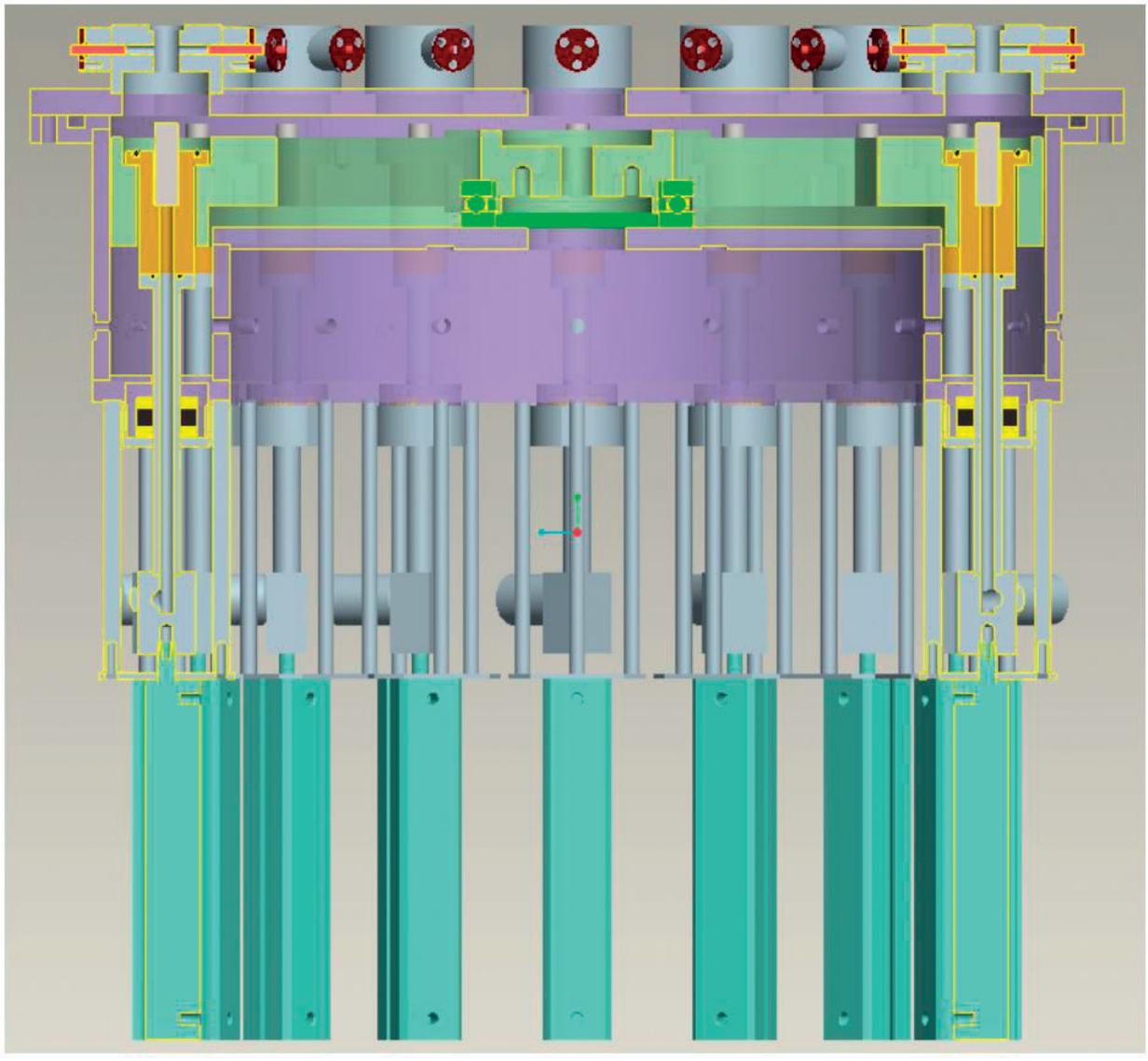

Figure 12. Design of sample distribution machine 'carousel'.

ones for neutron activation analysis, but other types of detector can be also considered. Appropriate detectors will be chosen for the proper operation of ITER NAS considering state of the art.

6. Performance assessment

The NAS system has been designed for determining the total neutron yield during the DT operation. The system must provide also time-resolved measurements of the global neutron source strength and evaluation of the fusion power. Measurement of absolutely calibrated neutron flux and fusion power will be performed.

Various tools are used for carrying out the analysis:

- MCNP v.5 (Monte Carlo N-Particle) transport code is used for the calculation of neutron fluxes and neutron energy spectra at the designated locations for the irradiation.
- FENDL-2.1 (Fusion Evaluated Nuclear Data Library) is used as the material database for the MCNP calculation
- FISPACT-2007 is used for the inventory of neutron induced activation of the sample materials.
- EAF-2007 (European Activation File) is used for the source of cross-section data for FISPACT-2007
- Lite series (A-lite, B-lite, and C-lite) 40° sector ITER geometrical model with a fusion plasma neutron source is used for the MCNP calculation.

An irradiation location at midplane inboard region is selected for the calculation of neutron flux and spectrum with MCNP code. The flux of this location is the second strongest among seven poloidal irradiation locations. Two tallies are designated for the irradiation ends, one is very close to the first wall, and the other is behind the blanket module very close to the

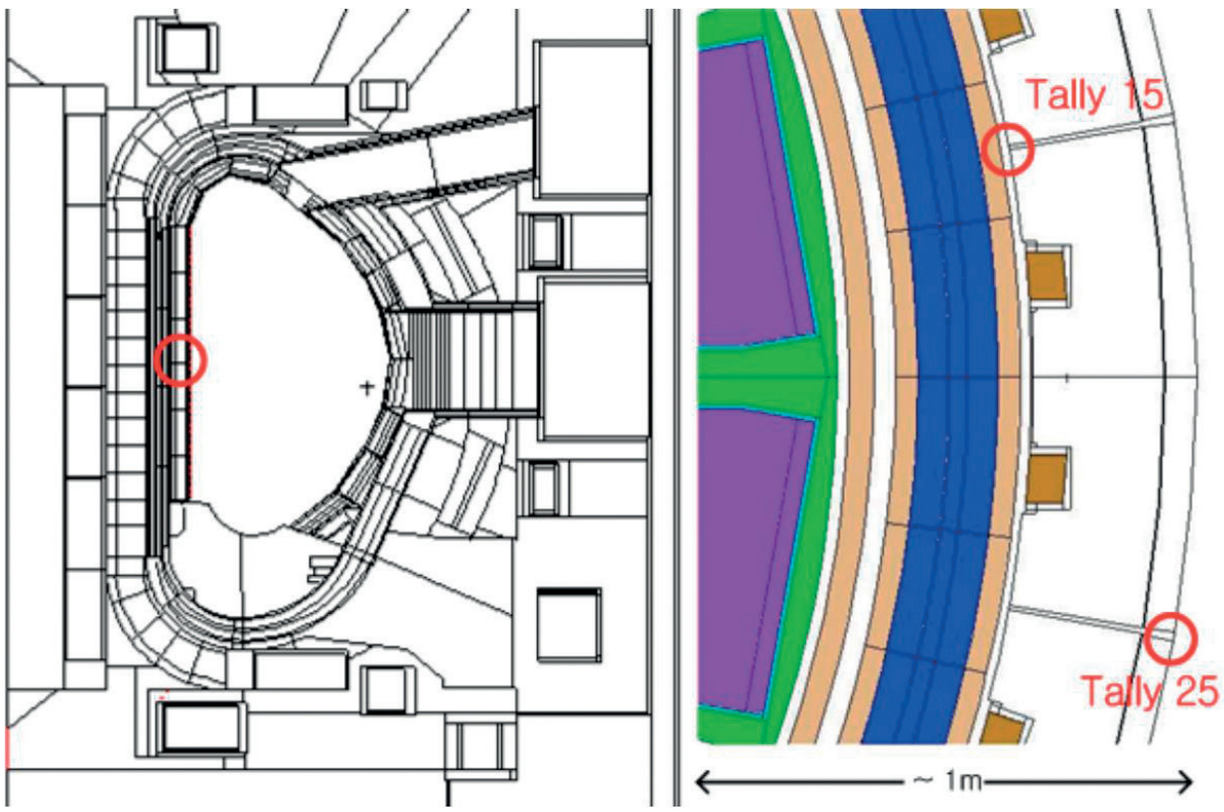

Figure 13. Tally locations in the Alite model.

vacuum vessel wall. Both are located at the cross point of horizontal and vertical gap centers of four blanket modules. Tally 15 is located near the inner VV wall whereas Tally 25 is facing the plasma. **Figure 13** shows two tally locations. Si, Al, Ti, Fe, Nb, and Cu have been selected as sample materials for the investigation [6]. Samples are assumed to be a foil type with the diameter of 7 mm and the thickness of 0.1 mm.

Figure 14 shows the calculated neutron spectra at two tallies. Total neutron fluxes at tally 15 and tally 25 are 5.45 × 1013 and 5.9 × 1014 s^{-1} cm^{-2} respectively, assuming 500 MW of fusion power. In spite of the heavy blanket modules structure in front of the irradiation end, the spectrum of tally 15 shows clear 14 MeV neutron peak. This is due to the blanket modules acting as a collimator that absorbs scattered neutrons. Calculated neutron flux and spectrum are used for input data of FISPACT for the calculation of the sample activity.

As one of the requirements of the ITER NAS is to measure time-integrated neutron fluence to the first wall for all discharge duration, it is desirable for samples to be irradiated as long as possible time within the discharge time. Thus, the activities of various samples are calculated with the irradiation of 1000 s, and the result is shown in **Figure 15** D-T fusion power of 500 MW is assumed for the flux calculation.

Another requirement is to provide supplementary neutron flux data with a crude temporal resolution of about 10 s, when necessary for a backup or calibration of other flux measurement systems, such as Microfission Chambers (MFC) and neutron flux monitors (NFM). Thus, the activities of various samples are calculated with the irradiation of 10 s, and the result is shown in **Figure 16**.

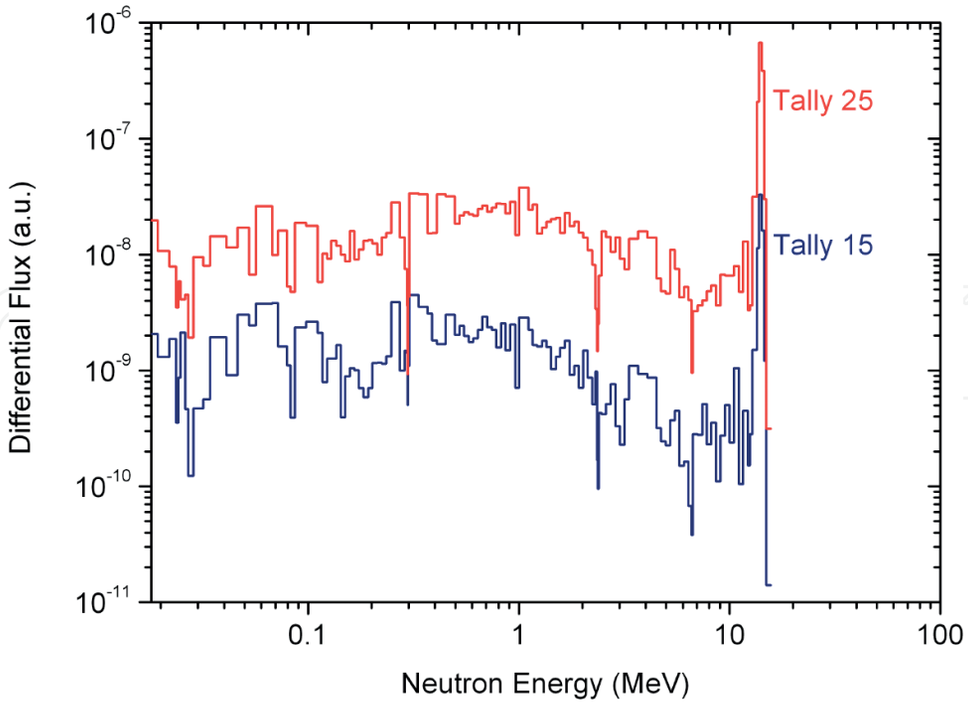

Figure 14. Neutron spectra at tally 15 and tally 25.

The activation desired for a sample should be similar to that provided by a standard source used for absolute calibration of the gamma-ray detectors. A typical maximum value for modestly safe handling would be 100 μCi. **Figure 17** shows the fusion power needed to create 100 μCi samples assuming 10-s irradiation and 20-s cooling at a irradiation location D.

Assuming the mass of samples to be from a few milligrams to a few grams, the fusion power that NAS can cover ranges from a few hundred watts to gigawatts by using various sample materials at different irradiation end locations. This measurement range satisfies the required measurement range both of the neutron flux and the fusion power.

Figure 18 shows the fusion power needed to create 100 μCi samples assuming 1000-s irradiation and 1000-s cooling at an irradiation location D. This result also shows that the NAS can measure neutron fluence in a long pulse operation condition of ITER. Si is not an appropriate sample material for the long time irradiation because the activity of Si saturates when the irradiation is much longer than the half-life of Si.

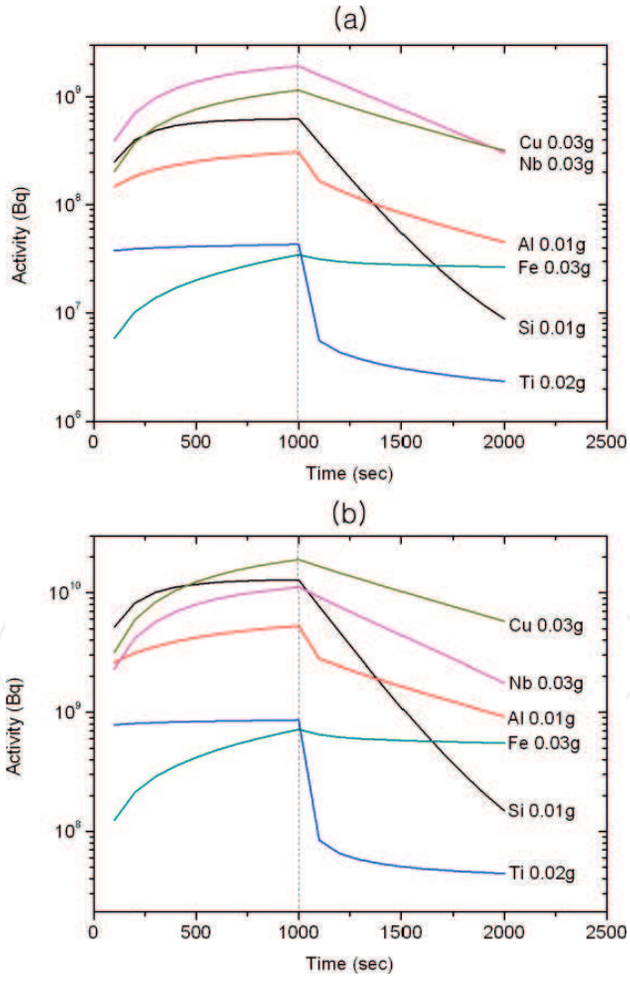

Figure 15. Activation by irradiation of 1000 s (a) tally 15, (b) tally 25.

http://dx.doi.org/10.5772/intechopen.75966

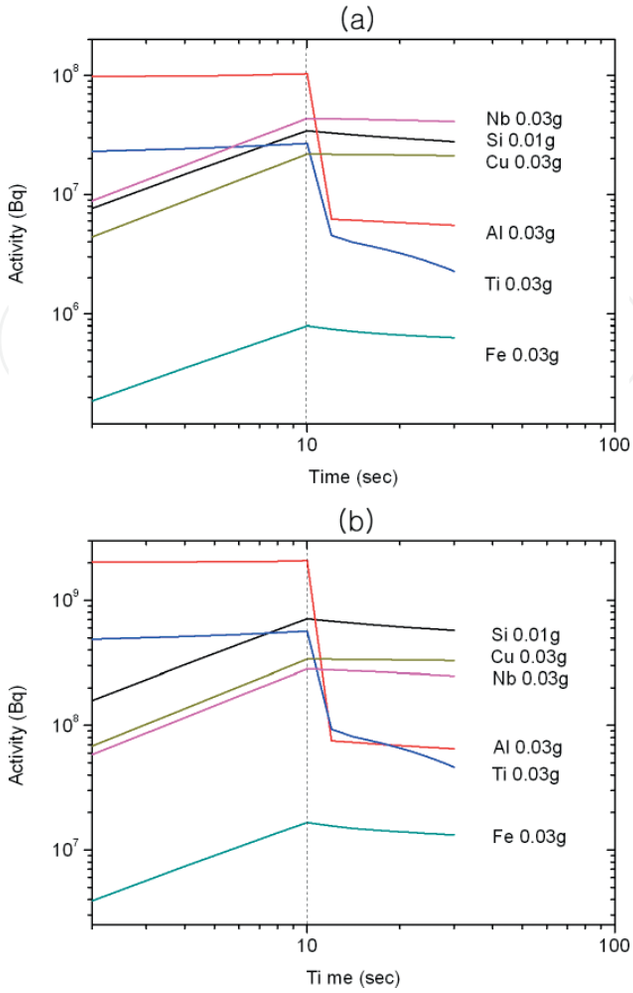

Figure 16. Activity by irradiation of 10 s (a) tally 15, (b) tally 25.

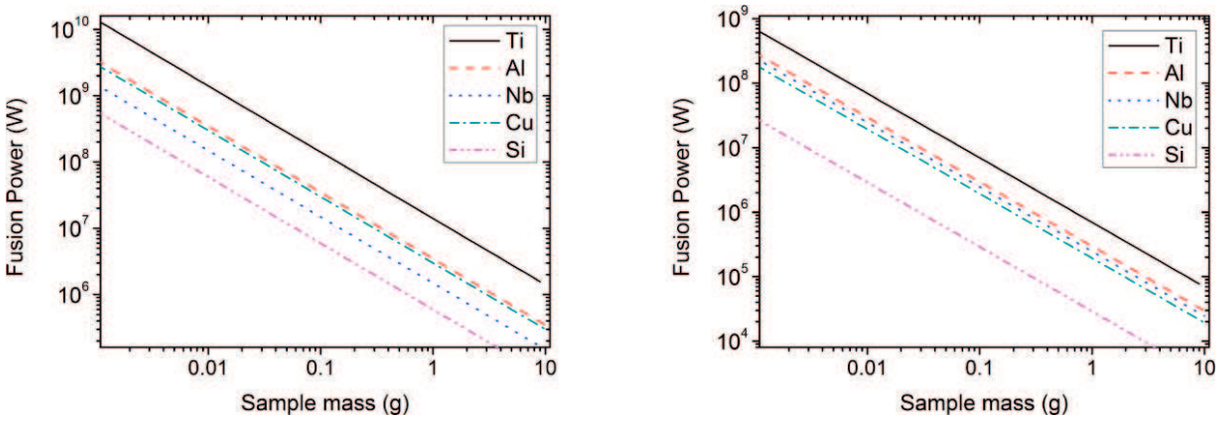

Figure 17. Fusion power needed to create 100 μCi samples by the 10-s irradiation and 20-s cooling (left) at tally 15, and (right) at tally 25.

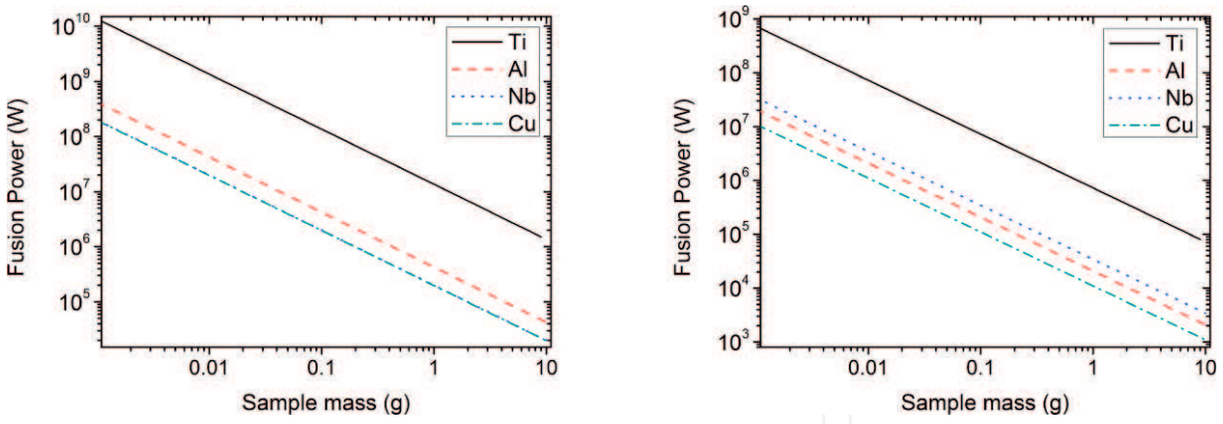

Figure 18. Fusion power needed to create 100 μCi samples by the 1000-s irradiation and 1000-s cooling (left) at tally 15, and (right) at tally 25.

7. Summary

The ITER neutron activation system that has been briefly presented in the earlier sections is under development by the Korean Domestic Agency of ITER. Despite the challenges driven by ITER's unprecedented thermal, electromagnetic and nuclear loads, those driven by high activation in full-power operation leading to very limited personnel access and the highest safety and reliability requirements [7], despite all these aspects, the presented NAS design proves to be suitable to satisfy ITER's measurement requirements.

Author details

Vitaly Krasilnikov[1,3]*, MunSeong Cheon[2] and Luciano Bertalot[1]

*Address all correspondence to: vitaly.krasilnikov@iter.org

1 ITER Organization, St. Paul-lez-Durance, France

2 National Fusion Research Institute, Daejeon, Republic of Korea

3 Tokamak Energy Ltd, Abingdon, UK

References

[1] Krasilnikov A et al. Status of ITER neutron diagnostic development. Nuclear Fusion. 2005;**45**:1503-1509

[2] Cheon MS, Pak S, Lee HG, Bertalot L, Walker C. In-vessel design of ITER diagnostic neutron activation system. Review of scientific instruments. 2008;**79**(10):10E505. DOI: 10.1063/1.2990857

[3] Cheon MS, Seon CR, Pak S, Lee HG, Bertalot L. Development of the prototype pneumatic transfer system for ITER neutron activation system. Review of Scientific Instruments. 2012;**83**(10):10D303. DOI: 10.1063/1.4729673

[4] Barnes CW, Loughlin MJ, Nishitani T. Neutron activation for ITER. The Review of Scientific Instruments. 1997;**68**:1-577. DOI: 10.1063/1.1147657

[5] Encheva A, Bertalot L, Macklin B, Vayakis G, Walker C. Integration of ITER in-vessel diagnostic components in the vacuum vessel. Fusion Engineering and Design. 2009;**84**:736-742

[6] Lee Y, Dang J, Jo J, Chun K, Hwang Y, Cheon M, Lee H, Bertalot L. Preliminary study on capsule material for ITER neutron activation system. Fusion Engineering and Design. 2014;**89**(9-10):1894-1898

[7] Vayakis G, Hodgson ER, Voitsenya V. Chapter 12: Generic diagnostic issues for a burning plasma experiment. Fusion Science and Technology. 2008;**53**:699-750

IntechOpen